



# LI-RADS version 2018 treatment response algorithm on extracellular contrast-enhanced MRI in patients treated with transarterial chemoembolization for hepatocellular carcinoma: diagnostic performance and the added value of ancillary features

Di Wang<sup>1,2</sup> · Yang Zhang<sup>2,3</sup> · Rong Lyu<sup>1</sup> · Kefeng Jia<sup>1</sup> · Peng-Ju Xu<sup>2,4</sup>

Received: 26 January 2024 / Revised: 3 March 2024 / Accepted: 3 March 2024 / Published online: 11 April 2024  
© The Author(s), under exclusive licence to Springer Science+Business Media, LLC, part of Springer Nature 2024

## Abstract

**Background** The Liver Imaging Reporting and Data System (LI-RADS) Treatment Response Algorithm (TRA) (LI-RADS TRA) is used for assessing response of HCC to locoregional therapy (LRT), however, the value of ancillary features (AFs) for TACE-treated HCCs has not been extensively investigated on extracellular agent MRI (ECA-MRI).

**Purpose** To evaluate the diagnostic performance of LI-RADS v2018 TRA on ECA-MRI for HCC treated with transarterial chemoembolization (TACE) and the value of ancillary features.

**Methods** This retrospective study included patients who underwent TACE for HCC and then followed by hepatic surgery between January 2019 and June 2023 with both pre- and post-TACE contrast-enhanced MRI available. Two radiologists independently evaluated the post-treated lesions on MRI using LI-RADS treatment response (TR) (LR-TR) algorithm and modified LR-TR (mLR-TR) algorithm in which ancillary features (restricted diffusion and intermediate T2-weighted hyperintensity) were added, respectively. Lesions were categorized as complete pathologic necrosis (100%, CPN) and non-complete pathologic necrosis (< 100%, non-CPN) on the basis of surgical pathology. The diagnostic performance in predicting viable and non-viable tumors based on LR-TR and mLR-TR algorithms was compared using the McNemar test. Interreader agreement was calculated by using Cohen's weighted and unweighted  $\kappa$ .

**Results** A total of 61 patients [mean age 59 years  $\pm$  10 (standard deviation); 47 men] with 79 lesions (57 pathologically viable) were included. For non-CPN prediction, the sensitivity, specificity of LR-TR viable and mLR-TR viable category were 75% (43 of 57), 82% (18 of 22) and 88% (50 of 57), 77% (17 of 22), respectively, the sensitivity of mLR-TR was significantly higher than that of LR-TR ( $P=0.016$ ) without difference in specificity ( $P=1.000$ ). Interreader agreement for LR-TR and mLR-TR category was moderate ( $k=0.50$ , 95% confidence interval 0.33, 0.67,  $k=0.42$ , 95% confidence interval 0.20, 0.63). The sensitivity of both LR-TR and mLR-TR algorithms in predicting viable tumors between conventional TACE (cTACE) and drug-eluting beads TACE (DEB-TACE) did not have significant difference (cTACE: 76%, 89% vs. DEB-TACE: 73%, 82%).

**Conclusions** On ECA-MRI, applying ancillary features to LI-RADS v2018 TRA can improve the sensitivity in predicting pathologic tumor viability in patients treated with TACE for hepatocellular carcinoma with no significant difference in specificity.

**Keywords** Hepatocellular carcinoma · Liver imaging reporting and data system (LI-RADS) · Treatment response · Washout

✉ Peng-Ju Xu  
xpjbf@163.com

<sup>1</sup> Department of Radiology, Tianjin Third Central Hospital, Tianjin Key Laboratory of Extracorporeal Life Support for Critical Diseases, Artificial Cell Engineering Technology Research Center, Tianjin Institute of Hepatobiliary Disease, No. 83 Jintang Road, Hedong District, Tianjin 300170, China

<sup>2</sup> Department of Radiology, Zhongshan Hospital, Fudan University, No. 180 Fenglin Road, Xuhui District, Shanghai 200032, China

<sup>3</sup> Department of Radiology, Dongying People's Hospital Shandong, Dongying, China

<sup>4</sup> Shanghai Institute of Medical Imaging, No. 180 Fenglin Road, Xuhui District, Shanghai 200032, China

## Abbreviations

AF	Ancillary feature
APHE	Arterial phase hyperenhancement
cTACE	Conventional TACE
CPN	Complete pathologic necrosis
DEB-TACE	Drug-eluting beads TACE
ECA	Extracellular contrast agent
HCC	Hepatocellular carcinoma
LI-RADS	Liver Imaging Reporting and Data System
LRT	Locoregional therapy
LR-TR	LI-RADS treatment response
NMLIT	Nodular, masslike, or irregular thick tissue in or along the treated lesions
TACE	Transarterial chemoembolization

## Introduction

Hepatocellular carcinoma is the sixth most commonly diagnosed cancer and the third leading cause of cancer-related deaths in the world, accounting for 75–85% of primary liver cancer, and its incidence is still expected to increase in the future [1].

Patients with HCC often undergo locoregional therapy (LRT) to downstage tumor as a bridge to liver transplant, resection or treatment for advanced disease. LRTs include ablation therapies (radiofrequency ablation, microwave ablation, percutaneous ethanol injection, and cryoablation), transcatheter therapies (transarterial embolization or transarterial chemoembolization, TACE) and radiation therapy (stereotactic body radiotherapy, SBRT) [2]. Of the LRTs, TACE is the most widely used as the first-line treatment for intermediate stage HCC according to the Barcelona Clinic Liver Cancer (BCLC) staging system [3]. After LRT, accurate assessment of viable tumors is crucial to guide further management. The concept of “LR-Treated” was first introduced in 2014 version of LI-RADS, in 2017, a dedicated treatment response algorithm was developed to provide an image-based assessment of HCC after locoregional therapy, and there was no modification of this algorithm in 2018 version of LI-RADS. The treated lesions are categorized to LR-TR viable, LR-TR equivocal and LR-TR nonviable according to contrast-enhanced CT/MRI features, including arterial phase hyperenhancement (APHE), washout, and enhancement similar to pretreatment enhancement [4]. Some recent studies have assessed the diagnostic performance of LR-TR v2018 after different LRTs [5–7], but most of them are based on MRI with hepatobiliary agent, HBA [8–10], the evidence of added value of ancillary features to LR-TR for TACE-treated HCC is insufficient, especially on ECA-MRI.

The purpose of this study was to assess the diagnostic performance of LR-TR v2018 algorithm and the value of ancillary features for HCC treated with TACE.

## Methods

Institutional Review Board in our hospital approved this retrospective study. The requirement for written informed consent was waived.

### Study population

We retrospectively reviewed electronic pathology records in our hospital (a tertiary care center) to search consecutive HCC patients (age  $\geq 18$  years) who were first treated by TACE and subsequently underwent hepatic surgery (local hepatic surgery or liver transplantation) between January 2019 and June 2023 ( $n = 176$ ). The exclusion criteria were as follows: (a) underwent surgery or LRTs before baseline MRI ( $n = 9$ ), or combined treatment with TACE including ablation ( $n = 2$ ) and systemic treatment ( $n = 37$ ), (b) HCC was treated at an outside hospital with no pretreatment MRI available ( $n = 61$ ) or no posttreatment MRI examination prior to surgery ( $n = 4$ ), (c)  $> 30$  days between post-TACE MRI examination and surgery ( $n = 2$ ).

Clinical and laboratory data from electronic medical record were collected for each patient including age at time of TACE, sex, etiology of chronic liver disease, type of surgery, alpha-fetoprotein, and protein induced by vitamin K absence or antagonist-II level before TACE, type of TACE, interval days between post-treatment MRI and surgery.

### Reference standard

All lesions were confirmed by surgical histopathology. Reference standard for viable and nonviable tumors was based on histopathological results from pathologic reports. Tumor necrosis was categorized as complete pathologic necrosis (100%, CPN) and non-complete pathologic necrosis ( $< 100\%$ , non-CPN). For complete necrotic tumors, the pathologist could see the outlines of dead HCC cells which can confirm that they were treated-HCCs.

A radiologist with 10 years abdominal MRI experiences annotated each target lesion matched with pathologic results on pre- and post-treatment MRI examinations. For patients who had multiple sets of MRI before TACE, chosen the examination closest to TACE. For patients undergone multiple TACE treatments, chosen the examination after last TACE and closest to surgery.

### Imaging protocol on ECA-MRI

All patients underwent MRI examinations with 3.0-T scanners (Siemens Healthcare, Prisma and uMR770, United Imaging Healthcare, Shanghai, China). The protocol

included: spoiled gradient-echo T1-weighted in/opposed phase imaging, turbo spin-echo T2-weighted imaging (T2WI), diffusion-weighted imaging (DWI,  $b$  values = 0, 50, and 500 s/mm<sup>2</sup>) and apparent diffusion coefficient (ADC) map, dynamic contrast-enhanced imaging using a T1-weighted, fat-suppressed sequence. The arterial, portal venous, and delayed phase images were obtained respectively at 20–30 s, 70–90 s, and 180–300 s. The gadopentetate dimeglumine (Gd-DTPA) was administered intravenously at a rate of 2 mL/s and a dose of 0.1 mmol/kg, followed by a 20 mL saline flush. Scanning sequence parameters are summarized in Table E1.

### TACE procedure

Both cTACE and DEB-TACE were performed by selectively introducing a catheter into vessels feeding the tumor through a right femoral artery access. cTACE was performed by injecting a mixture of an iodized oil (4–20 mL, Lipiodol) and antineoplastic drugs followed by gelatin sponge particles. DEB-TACE was performed by using drug-eluting beads with diameters ranging from 100 to 300  $\mu$ m loaded with antineoplastic drugs.

### Imaging analysis

Two radiologists with 10 and 14 years of abdominal MRI experience (reader 1 Di Wang and reader 2 Yang Zhang) who knew the target observations but blinded to the pathologic results independently assessed the pre- and post-treatment images and categorized all lesions by using the LI-RADS v2018 (pre-TACE), LR-TR and mLR-TR algorithm (post-TACE). On pre-TACE images, readers assessed tumor location and size, then gave the category of LI-RADS based on major features only, including nonrim arterial phase hyperenhancement (APHE), non-peripheral washout and enhancing capsule appearance. On post-TACE images, readers assessed the whole tumor size and viable/equivocal tumor size, then assigned a category by using LR-TR and modified LR-TR algorithm, respectively. The lesion was categorized as LR-TR viable, LR-TR nonviable and LR-TR equivocal on basis of the LR-TR algorithm, LR-TR viable had nodular, masslike, or irregular thick tissue in or along the treated lesion (NMLIT) with any of the following: (a) arterial phase hyperenhancement or (b) washout appearance or (c) enhancement similar to pretreatment. Washout was defined as reduction in enhancement relative to liver tissue in portal venous phase or delayed phase. Enhancement similar to pretreatment was defined as the observation had the same enhancing pattern with baseline images in all contrast enhancement phases. LR-TR nonviable showed no lesional enhancement or treatment-specific expected enhancement pattern (i.e., a thin smooth rim of enhancement surrounding

a non-enhancing lesion or typical treatment-related changes in parenchymal perfusion); LR-TR equivocal had atypical for treatment-specific expected enhancement pattern and not meeting criteria for probably viable or definitely viable. The mLR-TR criteria for viable category were as follows: (a) meet the LR-TR viable criteria; (b) NMLIT with indeterminate enhancement or no enhancement plus two ancillary features (restricted diffusion and intermediate T2-weighted hyperintensity), restricted diffusion defined as DWI hyperintensity at high  $b$  value or low ADC. Otherwise, the lesion was categorized as mLR-TR nonviable. The consensus reading was provided by a third radiologist (reader 3 with 28 years of abdominal MRI experience Peng-ju Xu).

### Statistical analysis

Quantitative variables (age) consistent with normal distribution were expressed as mean  $\pm$  standard deviation, variables (tumor size, laboratory data, interval days) not consistent with normal distribution were expressed as median and range (minimum and maximum). Qualitative variables (sex, etiology, LI-RADS and LR-TR categories, type of surgery, type of TACE) were expressed as frequencies and percentages.

The diagnostic performance including sensitivity, specificity, accuracy of LR-TR and mLR-TR for predicting viable and nonviable tumors was compared in consensus by using the McNemar test with pathological results as a reference standard. For each post-TACE MRI feature, the sensitivity, specificity, positive predictive value (PPV), negative predictive value (NPV), and accuracy for the diagnosis of viable tumors were calculated. Interreader agreement for post-TACE assessment categories and MRI features was computed using Cohen's weighted  $\kappa$  [viable (score 1) vs. equivocal (score 0.5) vs. nonviable (score 0)] and unweighted  $\kappa$  with 95% confidence intervals, the  $\kappa$  value was interpreted as slight (0.01–0.20), fair (0.21–0.40), moderate (0.41–0.60), substantial (0.61–0.80), or almost perfect (0.81–1.00).

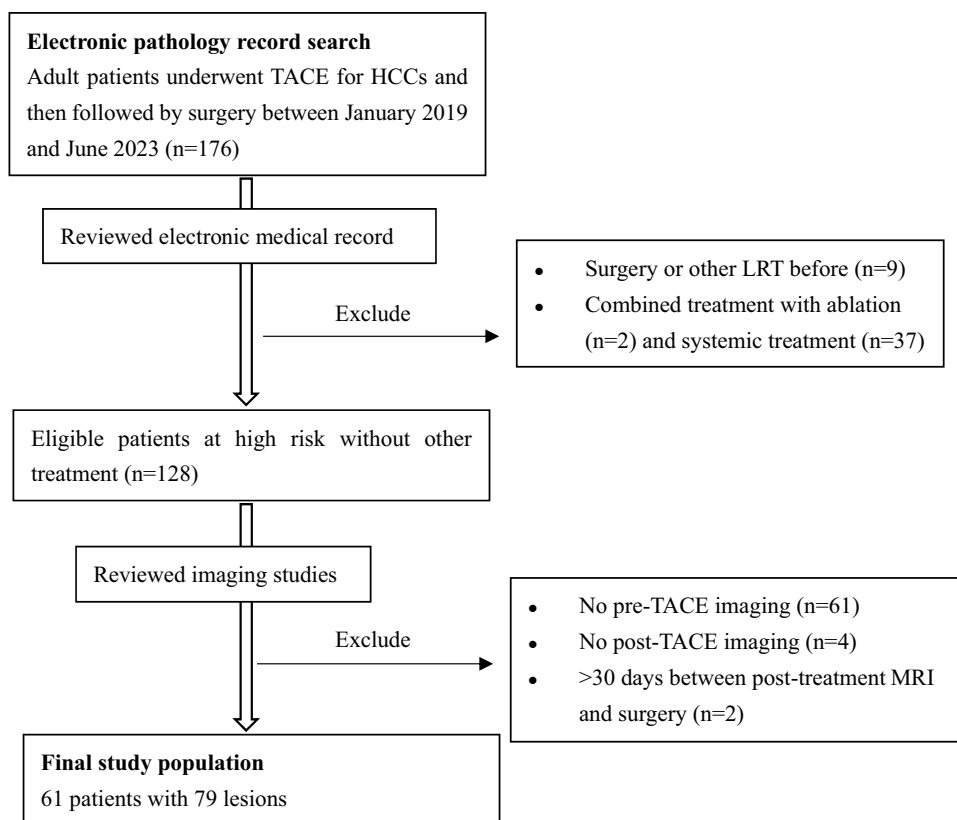
SPSS software (for Windows, version 26.0, IBM Corp, USA) was used for all statistical analysis.  $P < 0.05$  indicated a significant difference.

## Results

### Patient characteristics

Our final study population consisted of 61 patients (mean age at TACE 59 years  $\pm$  10; 47 men) with 79 lesions. This included 14 women (23%, mean age, 60 years  $\pm$  7) and 47 men (mean age, 60 years  $\pm$  11, Fig. 1). Hepatitis B viral infection (87%, 53 of 61) was the predominant etiology of underlying liver disease. 47 (77%, 47 of 61) Patients had a

**Fig. 1** Study flowchart. TACE transarterial chemoembolization, HCC hepatocellular carcinoma, LRT locoregional therapy



single lesion, 11 (18%, 11 of 61) patients had two lesions, and 3 (5%, 3 of 61) patients had three or more lesions. Most patients (97%, 59/61) underwent hepatic resections and only two underwent liver transplantation. The median interval between post-MRI and hepatic surgery was 6 days (1–27 days). Consensus LI-RADS category assignments for pre-TACE MRI findings were as follows: 4 as LI-RADS 4, 75 as LI-RADS 5. The majority (81%, 64 of 79) of lesions had been treated with conventional TACE, and the remaining 15 (19%, 15 of 79) lesions had been treated with DEB-TACE. 65 Lesions underwent one time TACE treatment, 12 lesions underwent two times TACE treatment, and 2 lesions underwent three times TACE treatment. The pre-TACE characteristics of patients are summarized in Table 1.

### Category assignment according to LR-TR and modified LR-TR Algorithms

On histopathology, 57 lesions were confirmed to be non-complete pathologic necrosis (non-CPN), and the remainder were confirmed to be complete pathologic necrosis (CPN). By consensus, 47 (59%, 47 of 79) of treated lesions were categorized as LR-TR viable, with 43 (91%, 43 of 47) lesions demonstrating non-CPN, 19 (24%, 19 of 79) of treated lesions were categorized as LR-TR nonviable, with 14 (74%, 14 of 19) lesions demonstrating CPN. 13 (16%, 13 of 79) of

treated lesions were categorized as LR-TR equivocal, with 9 lesions showing non-CPN and the other 4 showing CPN. According to the mLR-TR algorithm adding ancillary features, in consensus, 7 of equivocal lesions were assigned to viable, all of these were incompletely necrosis on histopathology, 6 of LR-TR equivocal lesions were assigned to nonviable, and 4 lesions were completely necrosis on histopathology, the percentage of viable tumors were both less than 10% in 2 false negative lesions.

### Diagnostic performances of LR-TR and modified LR-TR algorithm

The diagnostic performance in predicting complete and incomplete tumor necrosis based on different algorithms is summarized in Table 2, each reader's performance is presented in Table E2 (online). For non-CPN prediction, the sensitivity, specificity and accuracy of LR-TR viable were 75% (43 of 57), 82% (18 of 22) and 77% (61 of 79) respectively when LR-TR equivocal category was treated as nonviable (Fig. 2). For CPN prediction, the sensitivity, specificity and accuracy of LR-TR nonviable were 64% (14 of 22), 91% (52 of 57) and 84% (66 of 79), respectively, when LR-TR equivocal category was treated as viable.

Compared to LR-TR v2018, the sensitivity of the mLR-TR version in predicting non-CPN increased from 75 to 88%

**Table 1** Patient characteristics prior to TACE

Characteristics	Value
Patient	<i>N</i> =61
Age at time of TACE (years) <sup>a</sup>	59 ± 10 (32–79)
Sex (male:female)	47:14
Etiology of liver disease <sup>c</sup>	
Hepatitis B	53 (86.9)
Hepatitis C	3 (4.9)
Alcoholic liver disease	2 (3.3)
Cirrhosis of unknown causes	3 (4.9)
AFP level (ng/mL) <sup>b</sup>	61 (1.4–60,500)
PIVKA-II level (mAU/mL) <sup>b</sup>	342 (12–75,000)
Type of surgery <sup>c</sup>	
Local resection	59 (96.7)
Liver transplantation	2 (3.3)
Interval between post-MRI and operation <sup>b</sup>	6 (1–27)
Characteristics	Value
Lesion: pre-TACE characteristics	<i>N</i> =79
Type of TACE <sup>c</sup>	
Conventional TACE	64 (81.0)
DEB-TACE	15 (19.0)
Pretreatment LI-RADS category by consensus <sup>c</sup>	
LI-RADS 4	4 (5.1)
LI-RADS 5	75 (94.9)
Median size (mm) by consensus <sup>b</sup>	39 (6–158)

AFP alpha-fetoprotein, DEB-TACE drug-eluting beads TACE, LI-RADS Liver Imaging Reporting and Data System, PIVKA-II Protein Induced by Vitamin K Absence or Antagonist-II, TACE transarterial chemoembolization

<sup>a</sup>Data are mean ± standard deviation

<sup>b</sup>Data are medians, with ranges in parentheses

<sup>c</sup>Data are numbers, with percentages in parentheses

**Table 2** Diagnostic performances of treatment response algorithms in consensus reading in predicting histopathologic incomplete necrosis and complete necrosis

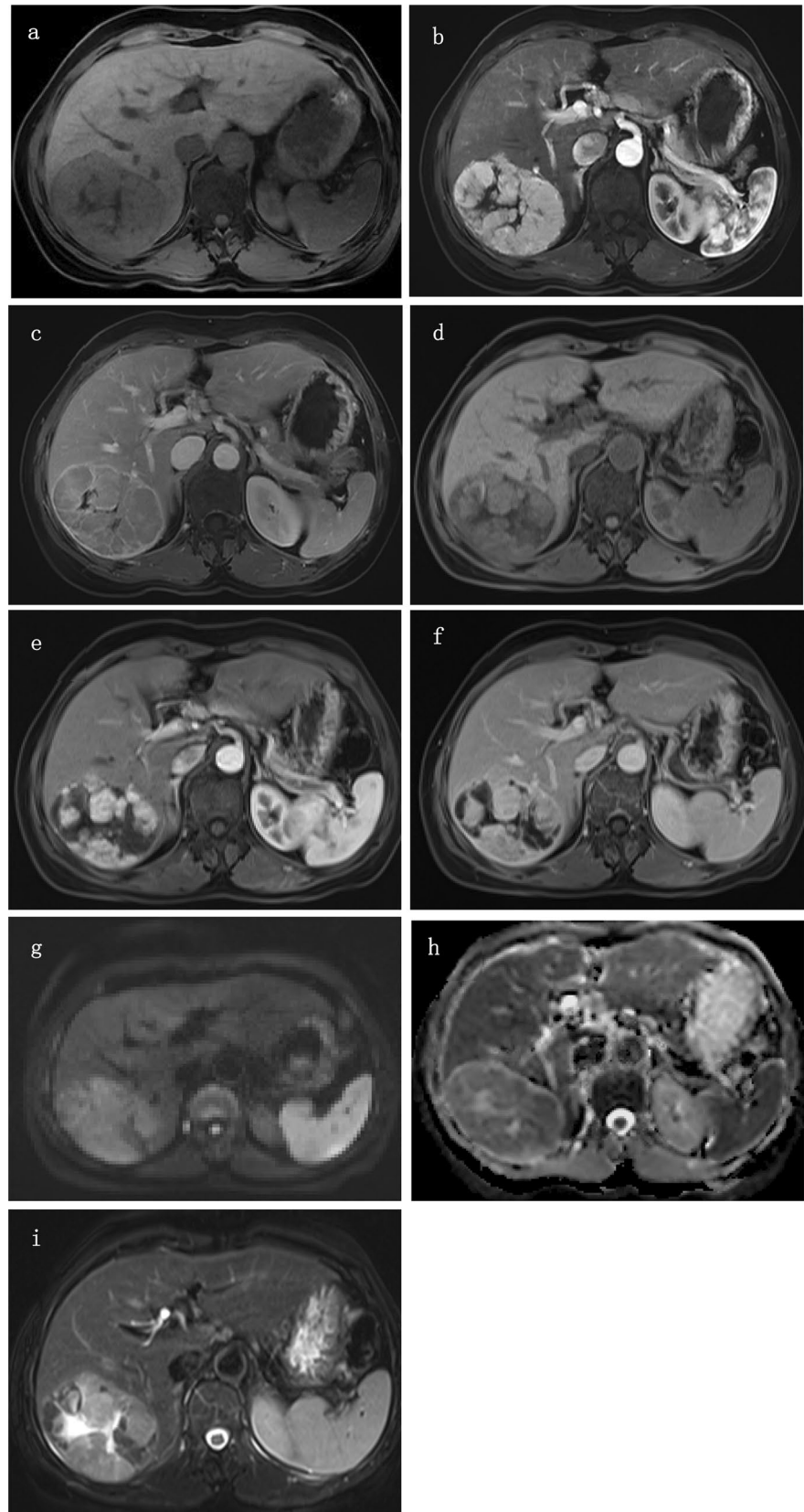
Assessment	Sensitivity (%)	Specificity (%)	Accuracy (%)
LR-TR viable (vs. nonviable and equivocal)			
LR-TR (equivocal as nonviable)	75 (43/57) [0.639, 0.870]	82 (18/22) [0.643, 0.993]	77 (61/79) [0.678, 0.867]
Modified LR-TR	88 (50/57) [0.789, 0.965]	77 (17/22) [0.583, 0.963]	85 (67/79) [0.798, 0.948]
<i>P</i> value	0.016	1.000	0.070
LR-TR nonviable (vs. viable and equivocal)			
LR-TR (equivocal as viable)	64 (14/22) [0.418, 0.855]	91 (52/57) [0.837, 0.988]	84 (66/79) [0.752, 0.915]
Modified LR-TR	77 (17/22) [0.583, 0.963]	88 (50/57) [0.789, 0.965]	85 (67/79) [0.798, 0.948]
<i>P</i> value	0.250	0.500	1.000

Data are percentages, with numbers of patients in parentheses; 95% confidence intervals are in brackets

LR-TR Liver Imaging Reporting and Data System Treatment Response

*P* values were obtained with McNemar test

**Fig. 2** 52-year-old woman with a history of hepatitis B infection. **a–c** MRI examination performed before treatment. Precontrast fat-suppressed T1-weighted image (**a**) shows an 8.6-cm hypointensity lesion in right posterior lobe of the liver with non-rim arterial phase hyperenhancement (APHE) in arterial phase (**b**) and non-rim washout as well as enhancing capsule in portal venous phase (**c**). According to Liver Imaging Reporting and Data System (LI-RADS) algorithm, this observation is categorized as LI-RADS 5. **d–i** MRI examination performed after conventional transarterial chemoembolization (cTACE). A 7.6-cm TACE-treated lesion shows hypointensity on precontrast fat-suppressed T1-weighted image (**d**) with nodular APHE in arterial phase (**e**) and persistent enhancement in delayed phase (**f**). The lesion is deemed as viable category according to LI-RADS Treatment Response algorithm (LR-TRA) by the presence of nodular APHE. The lesion shows restricted diffusion on diffusion-weighted image ( $b = 500 \text{ s/mm}^2$ ) (**g**) and ADC map (**h**), and intermediate hyperintensity on T2-weighted image (**i**) which also approve the viable diagnosis. Pathologic examination after surgery revealed noncomplete pathologic necrosis with a histological subtype of microtrabecular





(50 of 57) with  $P$  value = 0.016 (Fig. 3), the specificity was slightly decreased, with no statistical differences (77%, 17 of 22,  $P = 1.000$ ). For CPN prediction, the sensitivity of mLR-TR version was higher than LR-TR and the specificity was slightly decreased but both with no statistical differences ( $P = 0.250$  vs. 0.500). Interreader agreement of LR-TR and mLR-TR category was moderate ( $k = 0.50$ , [95% CI 0.33, 0.67],  $k = 0.42$ , [95% CI 0.20, 0.63]).

### Imaging features in predicting histological tumor viable

The diagnostic performance of each MRI feature is shown in Table 3, each reader's performance is presented in Table E (online). In terms of viable tumor prediction, among the LR-TR MRI features, NMLIT with APHE showed the highest sensitivity (72%, 41 of 57), while "NMLIT with washout" and "enhancing similar to pretreatment" showed the same specificity (86%, 19 of 22) which was slightly higher than "NMLIT with APHE" (82%, 18 of 22). The feature of "NMLIT with washout" ( $n = 25$ ) was mostly concomitance with that of "NMLIT with APHE" ( $n = 23$ ) and independently successfully predicted tumor viable in only two lesions. The feature of "NMLIT with enhancement similar to pretreatment" ( $n = 28$ ) did not change the categorization because it was mostly concomitance with that of "NMLIT with APHE" ( $n = 27$ ) or "NMLIT with washout" ( $n = 21$ ). For the ancillary features of mLR-TR, Intermediate hyperintensity on T2-weighted image showed high sensitivity (86%, 49 of 57) but low specificity (59%, 13 of 22). Restricted diffusion showed higher specificity (91%, 20 of 22) and slightly higher sensitivity (74%, 42 of 57) than NMLIT with APHE. Interreader agreement was moderate to substantial with  $\kappa$  values ranging from 0.56 to 0.66 for all assessed features.

### Discussion

Our results showed that the modified LR-TR algorithm had higher sensitivity in predicting viable tumors compared with the LR-TR algorithm when LR-TR equivocal category was treated as nonviable (88%, 50 of 57 vs. 75%, 43 of 57,  $P = 0.016$ ) and without significantly decreasing in specificity (77%, 17 of 22 vs. 82%, 18 of 22,  $P = 1.000$ ). The results are in accordance with some previous studies on the EOB-MRI-modified TR algorithm [8–10], in which AFs including not only "intermediate hyperintensity on T2-weighted image" and "restrict diffusion" but also "TP washout" and "HBP washout".

Compared with studies on EOB-MRI, our mLR-TR algorithm on ECA-MRI achieved comparable sensitivity with fewer AFs, which could be related to several possible reasons. First, our approach is strictly interpret the LR-TR algorithm by emphasizing the presence of nodular, mass-like, or irregular thick tissue morphology, even for ancillary features [11]. Second, the motion artifacts and weak enhancement in arterial phase for HBA-MRI may affect the identification of APHE, therefore, using ECA rather than HBA-MRI as a follow-up imaging modality after LRT may be more useful [12, 13].

Our study had a specificity of 82% to 86% in predicting viable tumors, which was consistent with most previous studies, but lower than the result by Kim et al. with a specificity of 93.3% to 100% [9]. The difference could be related to different reference standard, Kim et al. adopt both histological and clinical follow-up as reference standards, resulting in a significantly higher proportion of CPN (54%, 99 of 183) than in our study cohort (28%, 22 of 79) and most previous studies [5, 8, 11].

The interreader agreement was moderate for LR-TR category and mLR-TR category, which is accordance with previous studies [5, 11]. The variability in interreader agreement may be related to the following reasons. Despite the emphasis on NMLIT morphology, it is sometimes difficult to identify irregular thick tissue along the treated lesion, in addition, the judgment of indeterminate enhancement is different between readers. The interreader agreement of all posttreatment MRI features was similar ( $k$  range 0.56–0.66), and readers had the highest agreement regarding the feature of NMLIT with APHE ( $k = 0.66$ ), which is consistent with previous studies [5, 7, 11].

The sensitivity of NMLIT with washout in previous studies varied widely, ranging from 12.8 to 73% [8, 9, 11, 14], which may be related to different imaging modalities and different type of LRT. Our study had a sensitivity of 39%, which was lower than that of majority of studies. For viable tumors after treatment, the proportion of lesions (49%, 20 of 41) demonstrating both "NMLIT with APHE" and "NMLT with washout" was lower than pretreatment lesions (88%, 57 of 65), in the lesions demonstrating APHE but not showing washout after TACE, the observations were presented as isointensity (13 of 21) or hyperintensity (8 of 21) in delayed phase, while 17 of 21 ones showed washout on baseline MRI. The persistent enhancement manifestation was more common in the DEB-TACE group, accounting for 75% (6 of 8), which was much higher than in cTACE group (45%, 15 of 33). The result was consistent with the work by Adam et al.,

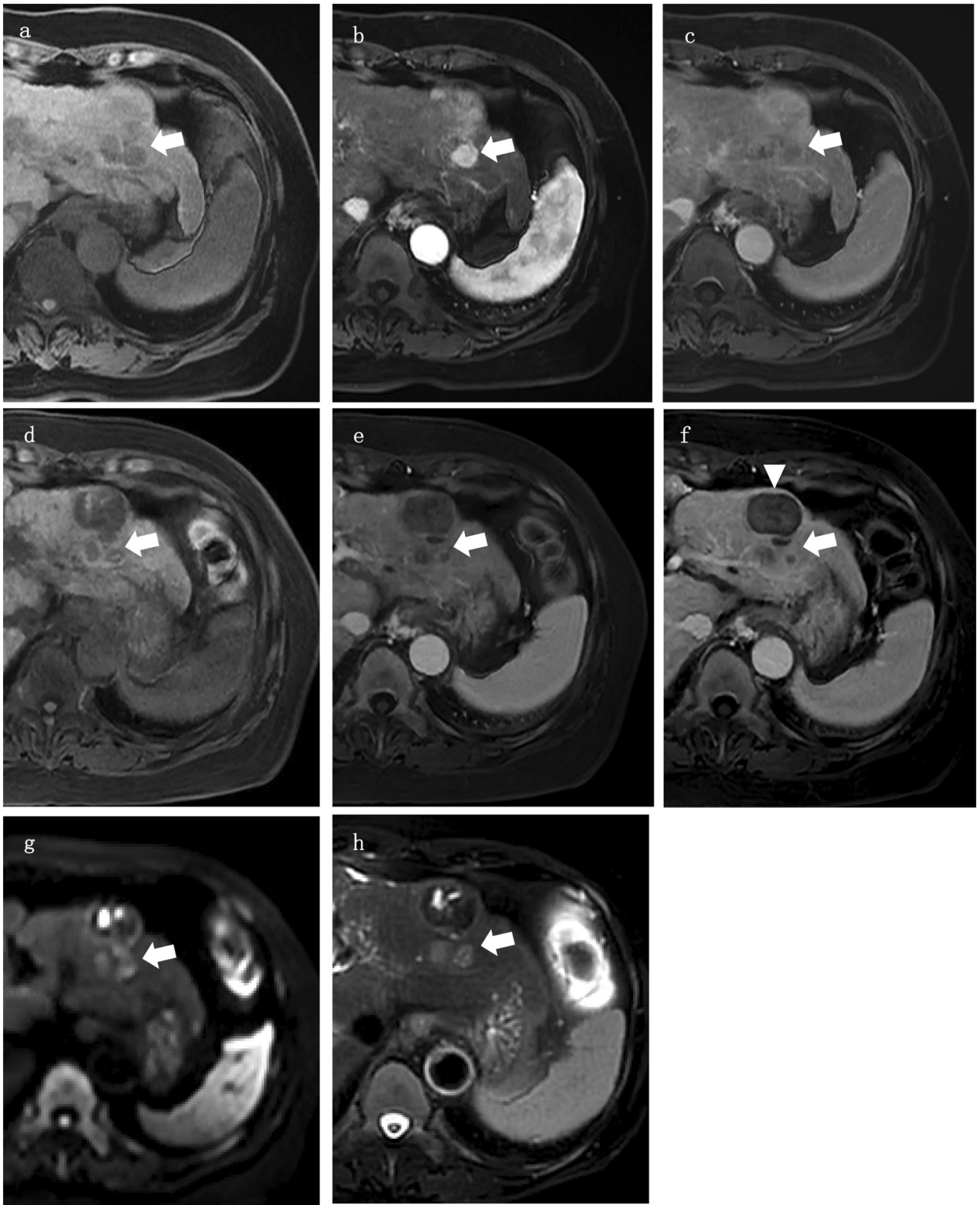




**Fig. 3** 61-year-old woman with cirrhosis due to hepatitis B infection. **a–c** MRI examination performed before treatment. Precontrast fat-suppressed T1-weighted image (**a**) shows a 2.8-cm hypointensity lesion (arrow) in left lobe of the liver with nodular APHE in arterial phase (**b**) and washout in delayed phase (**c**) that is assigned a LI-RADS 5 category. **d–h** MRI examination performed after cTACE. A 2.9-cm TACE-treated lesion shows hypointensity on precontrast fat-suppressed T1-weighted image (**d**) with indeterminate enhancement in arterial phase (**e**) and delayed phase (**f**) that is deemed LR-TR equivocal category. The lesion shows hyperintensity on diffusion-weighted image ( $b=500 \text{ s/mm}^2$ ) (**g**) and intermediate hyperintensity on T2-weighted image (**h**), the findings of these ancillary features support a modified LR-TR viable category. Pathologic examination after surgery revealed noncomplete pathologic necrosis. There was the other LI-RADS 5 lesion in left lobe of the liver with no enhancement after TACE (arrowhead in **f**) which revealed complete pathologic necrosis after surgery

who found only 18.8% of cases with baseline washout also showed washout on post-treatment imaging [15]. The persistent enhancement may represent fibrosis as a response to tissue injury and repair [2], further investigations are needed to confirm the precise mechanism.

In our study, the presence of “NMLIT with enhancement similar to pretreatment” did not change the categorization because these features were concurrent with APHE or washout which was in accordance with some previous studies [5, 7, 8, 16]. This finding may have significant implications for future revisions of the LI-RADS TR algorithm [17].

There is no demonstrable difference in tumor response or posttreatment appearances between cTACE and DEB-TACE

on MRI, but the ethiodized oil agent deposition in the tumor could influence the evaluation of posttreatment enhancement on CT [18–20]. Our result also showed the sensitivity of both LR-TR and mLR-TR algorithms in predicting viable tumors between cTACE and DEB-TACE did not have significant difference (cTACE: 76%, 89% vs. DEB-TACE: 73%, 82%).

There were some limitations in our study. First, our data was selected from a single tertiary care center with a relatively small sample, especially the patients underwent DEB-TACE treatment. In the future, more cases will be collected in multiple centers. Second, we only assessed the performance of ECA-MRI and did not compare with other imaging modalities such as contrast-enhanced CT and hepatobiliary contrast agents MRI. Third, although we adopt histopathologic results as reference standard, it is difficult to match lesions on imaging with pathology for small foci viable tumors. In addition, a maximum interval of 30 days between post-treated MRI examination and resection might introduce selection bias.

In conclusion, applying ancillary features on ECA-MRA to LI-RADS v2018 TRA can improve the sensitivity to predict pathologic tumor viability in patients treated with TACE for hepatocellular carcinoma without a loss of specificity. For TACE-treated HCC, viable tumors demonstrating “NMLIT with APHE” do not always show “NMLIT with washout”. The feature of “NMLIT with enhancement similar to pretreatment” do not change the categorization.

**Table 3** Diagnostic performance and interreader agreement of imaging features for detection viable tumors in consensus reading

Imaging features	Sensitivity	Specificity	PPV	NPV	Accuracy	Interreader agreement
NMLIT with APHE	72 (41/57)	82 (18/22)	91 (41/45)	53 (18/34)	75 (59/79)	0.66 [0.50, 0.83]
NMLIT with washout	39 (22/57)	86 (19/22)	88 (22/25)	35 (19/54)	52 (41/79)	0.56 [0.36, 0.75]
NMLIT with enhancement similar to pretreatment	44 (25/57)	86 (19/22)	89 (25/28)	37 (19/51)	56 (44/79)	0.57 [0.39, 0.76]
NMLIT with intermediate hyperintensity on T2WI	86 (49/57)	59 (13/22)	84 (49/58)	62 (13/21)	78 (62/79)	0.57 [0.37, 0.78]
NMLIT with restricted diffusion	74 (42/57)	91 (20/22)	95 (42/44)	57 (20/35)	78 (62/79)	0.64 [0.46, 0.81]

Data are percentages, with numbers of patients in parentheses; 95% confidence intervals are in brackets

APHE arterial phase hyperenhancement, NMLIT nodular, masslike, or irregular thick tissue in or along the treated lesion, NPV negative predictive value, PPV positive predictive value T2WI T2-weighted imaging

**Supplementary Information** The online version contains supplementary material available at <https://doi.org/10.1007/s00261-024-04275-y>.

**Funding** This study was funded by Shanghai 2022 “Science and Technology Innovation Action Plan” Medical Innovation Research Special Project (Grant Number 22Y11910900), and Tianjin Key Medical Discipline (Specialty) Construction Project (TJYXZDXK-074C).

## Declarations

**Conflict of interest** The authors declare that they have no conflict of interest.

**Ethical approval** Ethical approval was waived by the Local Ethics Committee of Zhongshan Hospital Fudan University in view of the retrospective nature of the study and all the procedures being performed were part of the routine care.

**Informed consent** The Institutional Review Board approved this study and waived informed consent because of retrospective study.

## References

- Sung H, Ferlay J, Siegel RL, Laversanne M, Soerjomataram I, Jemal A, Bray F. Global Cancer Statistics 2020: GLOBOCAN Estimates of Incidence and Mortality Worldwide for 36 Cancers in 185 Countries. *CA Cancer J Clin*. 2021 May;71(3):209–249. <https://doi.org/10.3322/caac.21660>
- Kielar, A., Fowler, K. J., Lewis, S., Yaghami, V., Miller, F. H., Yarmohammadi, H., Kim, C., Chernyak, V., Yokoo, T., Meyer, J., Newton, I., & Do, R. K. (2018). Locoregional therapies for hepatocellular carcinoma and the new LI-RADS treatment response algorithm. *Abdominal Radiology (New York)*, 43(1), 218–230. <https://doi.org/https://doi.org/10.1007/s00261-017-1281-6>
- Reig, M., Forner, A., Rimola, J., Ferrer-Fàbrega, J., Burrel, M., Garcia-Criado, Á., Kelley, R. K., Galle, P. R., Mazzaferro, V., Salem, R., Sangro, B., Singal, A. G., Vogel, A., Fuster, J., Ayuso, C., & Bruix, J. (2022). BCLC strategy for prognosis prediction and treatment recommendation: The 2022 update. *Journal of Hepatology*, 76(3), 681–693. <https://doi.org/https://doi.org/10.1016/j.jhep.2021.11.018>
- Chernyak V, Sirlin CB (eds) (2018) The LI-RADS® v2018 Manual. American College of Radiology Committee on LI-RADS®. American College of Radiology, Virginia. <https://www.acr.org/-/media/ACR/Files/Clinical-Resources/LIRADS/LI-RADS-2018-Manual-5Dec18.pdf>
- Shropshire, E. L., Chaudhry, M., Miller, C. M., Allen, B. C., Bozdogan, E., Cardona, D. M., King, L. Y., Janas, G. L., Do, R. K., Kim, C. Y., Ronald, J., & Bashir, M. R. (2019). LI-RADS Treatment Response Algorithm: Performance and Diagnostic Accuracy. *Radiology*, 292(1), 226–234. <https://doi.org/https://doi.org/10.1148/radiol.2019182135>
- Mendiratta-Lala, M., Aslam, A., Maturen, K. E., Westerhoff, M., Maurino, C., Parikh, N. D., Sun, Y., Sonnenday, C. J., Stein, E. B., Shampain, K. L., Kaza, R. K., Cuneo, K., Masch, W., Do, R. K. G., Lawrence, T. S., & Owen, D. (2022). LI-RADS Treatment Response Algorithm: Performance and Diagnostic Accuracy with Radiologic–Pathologic Explant Correlation in Patients with SBRT-Treated Hepatocellular Carcinoma. *International Journal of Radiation Oncology, Biology, Physics*, 112(3), 704–714. <https://doi.org/https://doi.org/10.1016/j.ijrobp.2021.10.006>
- Chaudhry, M., McGinty, K. A., Mervak, B., Lerebours, R., Li, C., Shropshire, E., Ronald, J., Commander, L., Hertel, J., Luo, S., Bashir, M. R., & Burke, L. M. B. (2020). The LI-RADS Version 2018 MRI Treatment Response Algorithm: Evaluation of Ablated Hepatocellular Carcinoma. *Radiology*, 294(2), 320–326. <https://doi.org/https://doi.org/10.1148/radiol.2019191581>
- Park, S., Joo, I., Lee, D. H., Bae, J. S., Yoo, J., Kim, S. W., & Lee, J. M. (2020). Diagnostic Performance of LI-RADS Treatment Response Algorithm for Hepatocellular Carcinoma: Adding Ancillary Features to MRI Compared with Enhancement Patterns at CT and MRI. *Radiology*, 296(3), 554–561. <https://doi.org/https://doi.org/10.1148/radiol.2020192797>
- Kim, S. W., Joo, I., Kim, H. C., Ahn, S. J., Kang, H. J., Jeon, S. K., & Lee, J. M. (2020). LI-RADS treatment response categorization on gadoxetic acid-enhanced MRI: diagnostic performance compared to mRECIST and added value of ancillary features. *European Radiology*, 30(5), 2861–2870. <https://doi.org/https://doi.org/10.1007/s00330-019-06623-9>
- Kim, Y. Y., Kim, M. J., Yoon, J. K., Shin, J., & Roh, Y. H. (2022). Incorporation of Ancillary MRI Features into the LI-RADS Treatment Response Algorithm: Impact on Diagnostic Performance After Locoregional Treatment of Hepatocellular Carcinoma. *American Journal of Roentgenology*, 218(3), 484–493. <https://doi.org/https://doi.org/10.2214/AJR.21.26677>
- Kierans, A. S., Najjar, M., Dutruel, S. P., Gavlin, A., Chen, C., Lee, M. J., Askin, G., & Halazun, K. J. (2021). Evaluation of the LI-RADS treatment response algorithm in hepatocellular carcinoma after trans-arterial chemoembolization. *Clinical Imaging*, 80, 117–122. <https://doi.org/https://doi.org/10.1016/j.clinimag.2021.06.009>
- Motosugi, U., Bannas, P., Bookwalter, C. A., Sano, K., & Reeder, S. B. (2016). An Investigation of Transient Severe Motion Related to Gadoxetic Acid-Enhanced MR Imaging. *Radiology*, 279(1), 93–102. <https://doi.org/https://doi.org/10.1148/radiol.2015150642>
- Huh, Y. J., Kim, D. H., Kim, B., Choi, J. I., & Rha, S. E. (2021). Per-Feature Accuracy of Liver Imaging Reporting and Data System Locoregional Treatment Response Algorithm: A Systematic Review and Meta-Analysis. *Cancers*, 13(17), 4432. <https://doi.org/https://doi.org/10.3390/cancers13174432>
- Bae, J. S., Lee, J. M., Yoon, J. H., Kang, H. J., Jeon, S. K., Joo, I., Lee, K. B., & Kim, H. (2021). Evaluation of LI-RADS Version 2018 Treatment Response Algorithm for Hepatocellular Carcinoma in Liver Transplant Candidates: Intraindividual Comparison between CT and Hepatobiliary Agent-Enhanced MRI. *Radiology*, 299(2), 336–345. <https://doi.org/https://doi.org/10.1148/radiol.2021203537>
- Polikoff, A., Wessner, C. E., Balasubramanya, R., Dulka, S., Liu, J. B., Machado, P., Savsani, E., Lyshchik, A., Shaw, C. M., & Eisenbrey, J. R. (2022). Imaging appearance of residual HCC following incomplete trans-arterial chemoembolization on contrast-enhanced imaging. *Abdominal Radiology (New York)*, 47(1), 152–160. <https://doi.org/https://doi.org/10.1007/s00261-021-03298-z>
- Seo, N., Kim, M. S., Park, M. S., Choi, J. Y., Do, R. K. G., Han, K., & Kim, M. J. (2020). Evaluation of treatment response in hepatocellular carcinoma in the explanted liver with Liver Imaging Reporting and Data System version 2017. *European Radiology*, 30(1), 261–271. <https://doi.org/https://doi.org/10.1007/s00330-019-06376-5>
- Kim TH, Woo S, Joo I, Bashir MR, Park MS, Burke LMB, Mendiratta-Lala M, Do RKG. LI-RADS treatment response algorithm for detecting incomplete necrosis in hepatocellular carcinoma after locoregional treatment: a systematic review and meta-analysis using individual patient data. *Abdom Radiol (NY)*. 2021 Aug;46(8):3717–3728. doi: <https://doi.org/10.1007/s00261-021-03122-8>

18. Voizard, N., Cerny, M., Assad, A., Billiard, J. S., Olivie, D., Perreault, P., Kielar, A., Do, R. K. G., Yokoo, T., Sirlin, C. B., & Tang, A. (2019). Assessment of hepatocellular carcinoma treatment response with LI-RADS: a pictorial review. *Insights into Imaging*, 10(1), 121. <https://doi.org/https://doi.org/10.1186/s13244-019-0801-z>
19. Golfieri, R., Giampalma, E., Renzulli, M., Cioni, R., Bargellini, I., Bartolozzi, C., Breatta, A. D., Gandini, G., Nani, R., Gasparini, D., Cucchetti, A., Bolondi, L., Trevisani, F., & Precision Italia Study Group (2014). Randomised controlled trial of doxorubicin-eluting beads vs conventional chemoembolisation for hepatocellular carcinoma. *British Journal of Cancer*, 111(2), 255–264. <https://doi.org/10.1038/bjc.2014.199>
20. Kwan, S. W., Fidelman, N., Ma, E., Kerlan, R. K., Jr, & Yao, F. Y. (2012). Imaging predictors of the response to transarterial

chemoembolization in patients with hepatocellular carcinoma: a radiological–pathological correlation. *Liver Transplantation: Official Publication of the American Association for the Study of Liver Diseases and the International Liver Transplantation Society*, 18(6), 727–736. <https://doi.org/https://doi.org/10.1002/lt.23413>

**Publisher's Note** Springer Nature remains neutral with regard to jurisdictional claims in published maps and institutional affiliations.

Springer Nature or its licensor (e.g. a society or other partner) holds exclusive rights to this article under a publishing agreement with the author(s) or other rightsholder(s); author self-archiving of the accepted manuscript version of this article is solely governed by the terms of such publishing agreement and applicable law.